Proceedings of the EuroGNC 2013, 2nd CEAS Specialist Conference on
Guidance, Navigation & Control, Delft University of Technology, Delft,
The Netherlands, April 10-12, 2013

Flight Guidance and Control of a Tethered Glider in an Airborne Wind Energy Application

Sören Sieberling

Abstract One of the concepts of an upcoming technology known as airborne wind energy is the pumping kite system. The pumping kite system uses a conventional gliders to fly highly dynamic crosswind patterns downwind of a generator to which it is connected by a tether to harvest wind energy. Operating the pumping kite system requires a novel view on conventional flight control. A tether based reference frame is introduced that in effect decouples the longitudinal and lateral motion which can thereby be designed independently and thus allowing the highly dynamic motion of the glider to be controlled through simple control schemes. Furthermore the longitudinal motion is constrained through the tether of which the tangential velocity is controlled by the generator providing an additional control input besides the elevator to control longitudinal motion. Flight tests demonstrate that using the tether based flight control system reasonably simple and commonly used control methods provide satisfactory flight performance.

1 Introduction

Harvesting wind energy is being investigated for several decades with many interesting outcomes as a result, [6]. One of the concepts introduced by [3] in the early eighties, describes a technique using a tethered glider that drives a generator on the ground through tension in the tether. [3] refers to this concept as lift power, also known as pumping-kite power. Today the pumping-kite system represents a subset of airborne wind energy, which has been a growing industry in the past decade with the sole objective of outperform conventional wind turbines in terms of cost per unit of energy.

Sören Sieberling
Ampyx Power B.V., Lulofsstraat 55 - 13, 2521AL Den Haag, The Netherlands, e-mail: sieberling@ampyxpower.com

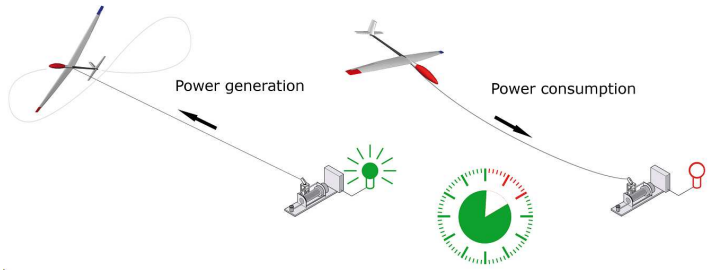

Fig. 1 The pumping kite system during power generation (left) and during reset (right).

The operational principle of the pumping kite system is discussed in Sec. 2, which is followed by Sec. 3 providing the physical framework. Sec. 4 presents the flight control system of the pumping kite system split into longitudinal and lateral control. Sec. 5 demonstrates some results from test flights, followed by the conclusions in Sec. 6.

2 Operational Principle of the Pumping Kite System

To convert wind into electrical energy the pumping kite system consists of an glider, a generator and a tether connecting the two. At the generator side the tether is wound on a drum that connects to the generator (together called winch). Lift is generated by flying crosswind patterns (similar to kites on a beach) downwind of the generator and transfered to the ground through tension in the tether that is experienced as torque by the generator.

The conversion of wind into electrical energy only takes place when the tether is unwound from the drum such that the lift can actually do work. Because of the tether being unwound, the operation of the pumping kite system consists of two phases; power generation and tether retrieval (reset), Fig. 1. When the maximum tether length is reached the glider changes its flight path from crosswind flight to flying straight toward the generator, while the tether is wound again. This tether retrieval maneuver results in low tether tension due to low drag, making the power consumption during tether retrieval significantly less than the power generated during the power generation phase at high tether tension due to high lift. This results in net power at the end of each power cycle.

One advantage of the pumping kite system compared to conventional wind energy becomes apparent when considering the wind power available, which is a function of ρ the air density and V_w the wind speed, Eq. 1.

$$P_\mathrm{w} = \frac{1}{2}\rho V_\mathrm{w}^3 \tag{1}$$

A specific device can generate more power than another by being located in an area with more wind (higher wind power density). The operational altitude of the pumping kite system is between 400 and 500 m. When assuming that the wind profile increases logarithmic with altitude [7, 4], wind power at for example 80 m hub height compared to 400 m doubles (above agricultural land). In terms of wind speeds this translates roughly into 25% wind speed increase.

A second advantage is that wind turbines are not expected to grow in the near future [5]. Consider that power is cubically related to airspeed. With airspeed over a wind turbine blade increasing linearly, it follows that most power in a wind turbine is generated by its blade tips. When assuming that the power generated by a section of the wind turbine blade is only a function of airspeed, hence neglecting the effect of airfoil and chord variation, almost 60% of the power would be generated by the outer 25% of the blades. In effect the pumping kite system could be compared to this outer section of the wind turbine blades. The difference to wind turbines is that it does not require a large tower and can operate with only one 'blade', thereby removing one of big upscaling obstruction of conventional wind turbines.

3 Physical Framework

The operation of the pumping kite system and the possible power output as a function of the wind speed is best described by basic aerodynamic equations and derivatives thereof, [3]. For simplicity the influence of mass on the system is neglected in these derivations. The glider is assumed to have no roll angle compared to the tether. And the wind is assumed to have a constant velocity, (V_w), parallel to the ground plain.

The lift generated by the glider is given by Eq. 2.

$$L = \frac{1}{2}\rho V_{\mathrm{TAS}}^2 S C_\mathrm{L} \tag{2}$$

With L the lift, V_{TAS} the true airspeed of the glider, S the wing surface area and C_L the lift coefficient. The drag of the system consists of two components, glider drag and tether drag. The drag of the glider is given by Eq. 3.

$$D_\mathrm{ac} = \frac{1}{2}\rho V_{\mathrm{TAS}}^2 S C_\mathrm{D} \tag{3}$$

With D_ac the glider drag and C_D the drag coefficient, approximated by

$$C_\mathrm{D} = C_{\mathrm{D}_0} + \frac{C_\mathrm{L}^2}{\pi A R e} \tag{4}$$

Where C_{D_0} represents the zero lift drag coefficient and the remaining term the induced drag with e the span efficiency factor and AR the aspect ratio. The tether

drag is approximated by assuming that the tether is straight, [2]. Since the lift of the glider is about one order of magnitude larger than the tether drag, the resulting errors are negligible. The effect of the true wind on the tether drag is also neglected. The drag of an infinitesimal section of the tether ds is given by Eq. 5.

$$\mathrm{d}D = \frac{1}{2}\rho V_{\mathrm{ds}}^2 C_{\mathrm{D_c}} t \mathrm{d}s \tag{5}$$

With $V_{\mathrm{d}s}$ the speed of an infinitesimal section of the tether, t the tether thickness and $C_{\mathrm{D_c}}$ the tether drag coefficient. By assuming a straight line (the speed changes linearly with position on the tether) the sectional speed is approximated by Eq. 6

$$V_{\mathrm{ds}} = \frac{s}{l} V_{\mathrm{TAS}} \tag{6}$$

With l the tether length. Substituting Eq. 6 into Eq. 5 and equating moments around the generator of the tether drag (integrated over the tether length) on one hand and a resulting force on the glider, the resulting tether drag is derived, Eq. 7, [2].

$$D_{\mathrm{c}} l = \int_0^l s \mathrm{d}D = \int_0^l s \frac{1}{2}\rho \left(\frac{s V_{\mathrm{TAS}}}{l}\right)^2 C_{\mathrm{D_c}} t \mathrm{d}s = \frac{1}{8}\rho V_{\mathrm{TAS}}^2 t l^2 C_{\mathrm{D_c}} \tag{7}$$

The lift to drag ratio (G) of the pumping kite system is then obtained by dividing Eq. 2 by Eq. 3 and Eq. 7 resulting in Eq. 8.

$$G = \frac{C_{\mathrm{L}}}{C_{\mathrm{D}} + \frac{t l C_{\mathrm{D_c}}}{4S}} \tag{8}$$

Where the right hand component of the denominator will also be referred to as effective tether drag coefficient. In a massless system, the system lift to drag ratio equals the ratio of forward and upward airspeed (Fig. 2), or in other words the lift to drag ratio describes the forward speed of the glider as a function of wind speed, tether angles and tether speed, Eq. 9.

$$V_{\mathrm{p}} = G(V_{\mathrm{w}} \sin\Theta \cos\Phi - V_{\mathrm{t}}) = G V_{\mathrm{eff}} \tag{9}$$

With V_{p} the forward speed, Θ the in the wind plane rotation of the tether (Fig. 3), Φ the out of the wind plane rotation of the tether (Fig. 3) and V_{t} the tether speed. Note that this equation holds only for a massless system, or in other words when the system is in equilibrium.

For rigid wing kites, the difference between V_{p} and V_{TAS} becomes negligible due to the high system lift to drag ratio, Eq. 10.

$$V_{\mathrm{TAS}} \approx V_{\mathrm{p}} \tag{10}$$

Furthermore, when assuming a high lift to drag ratio, the tether tension is approximately equal to the lift. With the tension then given, the resulting power during the power generating phase is computed by Eq. 11.

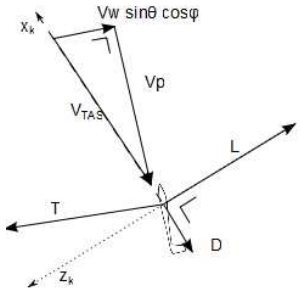

Fig. 2 Force and speed diagram during power production for forces in equilibrium, showing identical ratios between L/D and $V_p/V_w \sin\Theta\cos\Phi$. The dashed lines indicate the kinematic reference frame (X pointing in the direction of the airspeed).

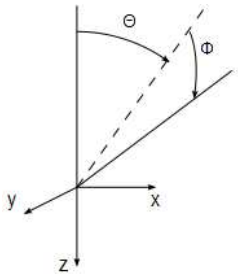

Fig. 3 Definition of tether angles with respect to wind direction blowing along the X-axis. Θ in the wind plane rotation and Φ out of the wind plane rotation.

$$P = \eta_{\mathrm{m}} T V_{\mathrm{t}} \tag{11}$$

With η_m the mechanical efficiency of the motor and other winch components. In the derivation above the tether speed has not been specified. [3] however demonstrates that for maximum power production the tether speed, should be 1/3 of the wind speed component perpendicular to the glider, thus $V_{\mathrm{w}} \sin\Theta\cos\Phi/3$.

Note that these derivations are a simple means to analyzing the pumping kite systems characteristics. The biggest assumption is that the system is massless. In reality the glider is constantly maneuvering to stay inside the wind window and thus constantly accelerating hence not being in equilibrium. The true motion is governed by the equations of motion conventional to aircraft, Eqs. 12.

$$\begin{bmatrix} \dot{u} \\ \dot{v} \\ \dot{w} \end{bmatrix} = \frac{1}{m} \begin{bmatrix} X \\ Y \\ Z \end{bmatrix} + g \begin{bmatrix} -\sin\theta \\ \sin\phi\cos\theta \\ \cos\phi\cos\theta \end{bmatrix} - \begin{bmatrix} p \\ q \\ r \end{bmatrix} \times \begin{bmatrix} u \\ v \\ w \end{bmatrix} \tag{12a}$$

$$\begin{bmatrix} \dot{p} \\ \dot{q} \\ \dot{r} \end{bmatrix} = J^{-1} \left(\begin{bmatrix} L \\ M \\ N \end{bmatrix} - \begin{bmatrix} p \\ q \\ r \end{bmatrix} \times \left\{ J \begin{bmatrix} p \\ q \\ r \end{bmatrix} \right\} \right) \tag{12b}$$

$$\begin{bmatrix} \dot{\theta} \\ \dot{\phi} \\ \dot{\psi} \end{bmatrix} = \begin{bmatrix} 1 & \sin\phi\tan\theta & \cos\phi\tan\theta \\ 0 & \cos\phi & -\sin\phi \\ 0 & \frac{\sin\phi}{\cos\theta} & \frac{\cos\phi}{\cos\theta} \end{bmatrix} \begin{bmatrix} p \\ q \\ r \end{bmatrix} \tag{12c}$$

$$\begin{bmatrix} V_{\mathrm{N}} \\ V_{\mathrm{E}} \\ V_{\mathrm{D}} \end{bmatrix} = T_{\mathrm{nb}} \begin{bmatrix} u \\ v \\ w \end{bmatrix} + \begin{bmatrix} V_{\mathrm{wind_N}} \\ V_{\mathrm{wind_E}} \\ V_{\mathrm{wind_D}} \end{bmatrix} \tag{12d}$$

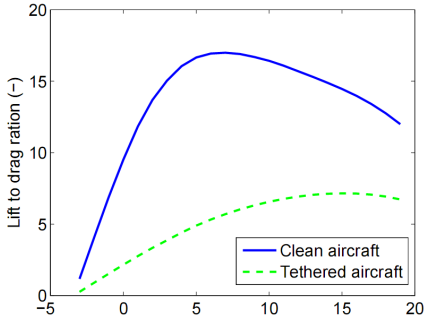

Fig. 4 The lift to drag ratio of a clean free flying glider vs angle of attack compared to the lift to drag ratio of a tethered glider with a fixed tether length of 400m vs. angle of attack.

With u, v, w velocity along respectively the body x, y, z axis, p, q, r rotational rates along respectively the body x, y, z axis, ϕ, θ, ψ the euler angles, V_{N}, V_{E}, V_{D} velocity respectivily north, east, down, g the gravitational constant, X, Y, Z, aerodynamics and tether forces along respectively x, y, z axis, L, M, N aerodynamic and tether moments around respectively the x, y and z axis and T_{nb} the transformation matrix from the body to the inertial reference frame, which can be found in any common book on aircraft dynamics.

When using the derivation as a qualitative means to describe the pumping kite system scaling, two observations can be made, [8]:

(A) From the discussion above it is concluded that when flying at higher lift to drag ratios the power output grows. Since not only the glider lift to drag ratio is of concern but the lift to drag ratio of the system, higher lift to drag ratio within operational flight envelopes almost always correspond to higher lift and therefor higher angle of attack, Fig. 4.

As is also stated by Eq. 9, higher lift to drag ratio also corresponds to higher true airspeed, which results in the unconventional flight characteristic for a tethered glider that the airspeed is raised by pitching up instead of pitching down.

(B) For free flying glider the lift to drag ratio provides a means to compare glider performance because it is dimensionless. For tethered glider the system lift to drag ratio is however not independent of dimension, meaning that system lift to drag ratios of differently sized systems should not be compared without corrections.

The scaling dependency of the system lift to drag ratio is caused by the tether dimensioning. When expressing the scaling of glider in terms of wing surface, twice as much wing surface results in twice as much lift and drag, hence tension. Twice the amount of tension requires twice the amount of tether, hence the tether cross-sectional surface doubles. Since the system lift to drag ratio does not depend on tether cross section but on tether diameter, the effective tether drag coefficient will

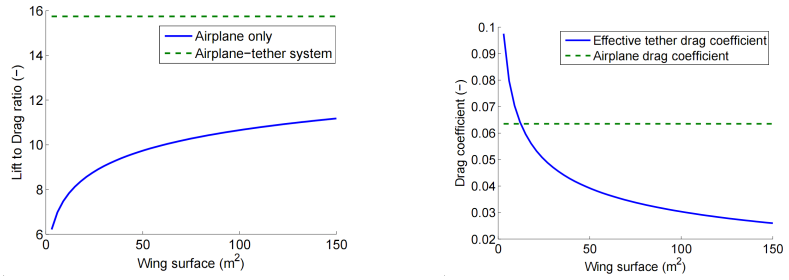

(a) Lift to drag ratio (b) Drag coefficient

Fig. 5 System lift to drag ratio and total drag coefficient as a function of glider dimension.

grow with the square root of the tether cross section, hence proportional to the square root of the wing surface. Therefore the relative contribution of the tether drag becomes smaller.

Fig. 5(a) illustrates the system lift to drag ratio of differently sized pumping kite systems having identical aerodynamic characteristics in terms of glider lift and coefficients. Furthermore the tether length is identical for different sizes. Sizing of the tether thickness is based on the tension at a fixed airspeed and lift. In reality the tether length will grow slightly for increasing systems as will airspeed, which would have a softening effect on the differences in system lift to drag ratio. Fig. 5(b) illustrates the glider and tether drag coefficients, which illustrates that the system lift to drag ratio grows for aerodynamically identical glider as the system is scaled up, thus tether drag is a bigger problem for smaller systems.

4 Guidance and Control

Compared to most conventional glider, the maneuvering of the pumping kite can be perceived as aggressive and nonlinear. In only a few seconds the roll angle changes from plus to minus 60°, while the heading is changing direction 180°and the pitch angle is going up and down from 60 to -20°.

When however changing the control reference to a tether based reference frame, the same maneuvers become rather mild and practically speaking linear in the sense that dynamic coupling can be neglected and longitudinal and lateral control can be separated. The tether based 'Euler' angles then vary only up to 20°for the roll and pitch angle.

The transformation from inertial reference frame to the tether based reference frame is defined by:

1. Rotation around the earth fixed Z-axis by Ψ, the wind direction, with corresponding direction cosine matrix $T_{Z(\psi)}$

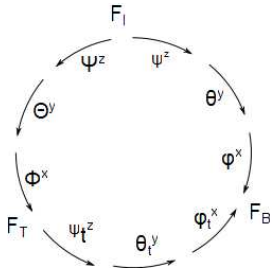

Fig. 6 Reference frame transformation summary. Reference frames are indicated by the capital letter F, with the subscript indicating the specific frame. Superscripts are used to indicate the axis of rotation.

2. Rotation around the Y-axis by $-\Theta$, with corresponding direction cosine matrix $T_{\mathrm{y}_{(-\Theta)}}$
3. Rotation around the X-axis by Φ, with corresponding direction cosine matrix $T_{\mathrm{x}_{(\Phi)}}$

$$C_{\mathrm{ti}} = T_{\mathrm{x}_{(\phi)}} T_{\mathrm{y}_{(-\theta)}} T_{\mathrm{z}_{(\psi)}} \tag{13}$$

With C_{ti} the direction cosine matrix mapping inertial coordinates into tethered coordinates and the other way around by taking the transpose, $C_{\mathrm{it}} = C_{\mathrm{ti}}^{\mathrm{T}}$. When introducing the conventional axis transformation from the inertial reference frame to the body fixed reference frame by means of the Euler angles (roll (ϕ), pitch (θ) and yaw (ψ)) as C_{bi}, the direction cosine matrix to the body frame from the tethered frame is given by Eq. 14.

$$C_{\mathrm{bt}} = C_{\mathrm{bi}} C_{\mathrm{it}} \tag{14}$$

The tethered Euler angles are then derived consequently as in Eqs. 15. The transformations are summarized in Fig. 6.

$$\phi_{\mathrm{t}} = \tan^{-1}\left(C_{\mathrm{bt}_{(2,3)}} / C_{\mathrm{bt}_{(3,3)}}\right) \tag{15a}$$

$$\theta_{\mathrm{t}} = \sin^{-1}\left(-C_{\mathrm{bt}_{(1,3)}}\right) \tag{15b}$$

$$\psi_{\mathrm{t}} = \tan^{-1}\left(C_{\mathrm{bt}_{(1,2)}} / C_{\mathrm{bt}_{(1,1)}}\right) \tag{15c}$$

4.1 Longitudinal Control

As is concluded in section 3, the crux for high power outputs is flying at high lift coefficients. Since the lift coefficient directly relates to angle of attack, this translates into a longitudinal control objective, being angle of attack tracking, which is

performed by the elevator. Angle of attack control alone is however not sufficient to control motion along the tether based Z-axis.

Another important, but unconventional factor to the longitudinal control of the pumping kite system is the constrained imposed by the tether. The motion along the direction of the tether (heave) is defined by the rotational velocity of the winch, which thereby becomes a second longitudinal control input. It is important to view the control on the glider and the control of the winch as one.

Both control inputs have effects on the tether tension. Lowering the angle of attack lowers the lift generation of the wing (hence tension), thereby also lowering the lift to drag ratio of the system (Fig. 4), which lowers the airspeed (which again lowers the tension). Raising the winch speed, lowers the effective wind at the plane, which lowers the airspeed and thereby the tension. It is not hard to understand that both control inputs in effect influence the same parameters, which can easily grow into instabilities. What makes this control problem more complicated is that communication between winch and glider is over radio suffering from transmission delays and that the winch has implementation delays orders of magnitude larger than the glider implementation delays.

4.1.1 Power Generation Phase

Mostly because of the system latencies the longitudinal control is chosen to use the elevator passively (in a fixed position comparable to a flap) and have the winch speed control the tether tension, by varying reel out speed. Simulations indicate that angle of attack control would become possible when latencies are reduced to about 50ms. Note that this implies not flying at the optimal $V_w/3$ as derived by [3]. By fixing the elevator in effect the angle of attack and thus the lift coefficient is set (and thus the lift to drag ratio). The winch is programmed to control the tension in the tether by varying the reel out speed, using a PI controller. The tension demand is scheduled with scheduled tension demand versus airspeed. The tension demand is scheduled such that at low airspeeds the tension demand rises, while at high airspeeds it drops. A rising tension demand will result in slower winch speed and thereby raising the effective wind experienced by the glider and visa versa.

Note that the winch control thereby does depend on the glider measurement by requiring information on the true airspeed. As mentioned before the communication between glider and winch uses radio and contains latencies, which is why the angle of attack is not controlled actively. Compared to angle of attack changes, the airspeed however changes orders of magnitude slower since physically it is a derivative of higher or lower lift to drag ratio in tethered flight. Therefor the system latencies are acceptable in this control architecture.

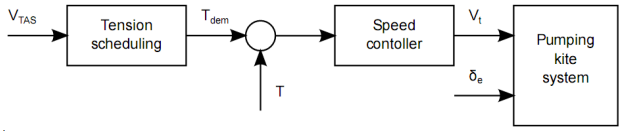

Fig. 7 Block diagram indicating the functioning of the longitudinal control scheme during power generation.

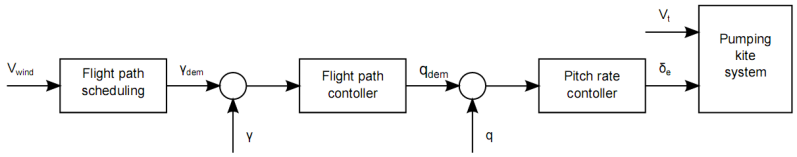

Fig. 8 Block diagram indicating the functioning of the longitudinal control scheme during system reset.

4.1.2 Reset Phase

As the tether length reaches its maximum the reset phase is triggered and activates a second set of longitudinal controls. In this setup the winch becomes the passive component by simply setting the winch speed to reeling in at maximum speed, thereby making the time for resetting the system as small as possible. The elevator is controlled to maintain a specific flight path angle that is derived from a sink demand setting, which is scheduled against wind speed.Since the winch speed in this phase is set, so is the ground speed. Which implies that the true airspeed, and thus the drag, rises with increasing wind. The scheduling is therefore chosen to have the reset phase consist of a steeper dive for higher wind speeds such that gravity compensates for the glider drag as much as possible, yet never makes it exceed the tether speed.

4.1.3 Phase Transitions

The change between control strategies is instant, therefore the plane enters the reset phase with a fast pitch down maneuver. The tether tension is thereby suddenly lowered and possibly the tether gets slack for a brief period. Shortly after the winch will however pick up the pace and straighten out the tether.

The transition back into the power generation flight path requires extra attention. The plane is flying into the wind at ground speeds roughly equal to the winch speed, such that the effective wind speed is that of the true wind plus that of the tether. The tether tension is low and approximately a full order of magnitude lower than during power generation. If the winch would respond too slow to the plane flying back into the pattern, considering the equations of Sec. 3, unfeasible airspeeds would arise. On the other hand if the winch responds too fast, the tension will drop completely and the plane would not make the turn back into the pattern at all, or it would build

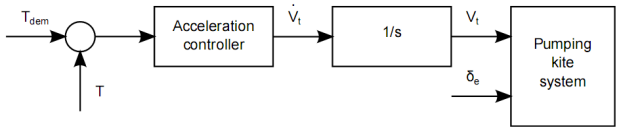

Fig. 9 Block diagram indicating the functioning of the longitudinal control scheme during transition into the power generation phase.

up momentum and at some point instantly tense the tether resulting in high shock loads. In other words the tether may not get slack, but it can also not build up tension, making the transition back into the pattern a delicate maneuver.

This creates hard requirements on the synchronisation, making the radio latencies unacceptable. For 'communication' in this situation the tether tension is therefor used. Yet switching back to the conventional tension controller is not an option since it is tuned to operate at reel out speeds during power generation and besides it would not be sensitive enough to responds to tension changes in the order of only 100N. Another simple controller is therefore designed, controlling the winch acceleration directly. The tension error that is measured with respect to a set reference tension, in the order of magnitude of the tension during the reset phase, is multiplied by a gain to yield the winch acceleration. This method, in combination with the fixed elevator, has proven to be fast and provides sufficient margin for different wind speeds.

4.2 Lateral Control

Essentially the lateral control is not much different as for conventional glider. The main difference compared to free flying glider is that the lateral control is not defined with respect to the inertial reference frame, but with respect to tether frame as defined in the beginning of this section.

The flight path is defined by waypoints in the spherical tether coordinates, Fig. 3, making the waypoints independent of tether length and wind direction. For flight guidance these spherical coordinates are mapped into the tether reference frame, with the origin in the generator, thereby generating waypoints in Cartesian coordinates. The tether coordinates of the flight path thereby do depend on wind direction and tether length (R), Eq. 16.

$$\begin{bmatrix} x \\ y \\ z \end{bmatrix}_{\mathrm{i}} = C_{\mathrm{it}} \begin{bmatrix} 0 \\ 0 \\ R \end{bmatrix}_{\mathrm{t}} \tag{16}$$

Different from the longitudinal control, only one controller governs the actual waypoint tracking. The lateral controller derives the closest point on the set flight path from its current position. Taking the closest point as a starting point a variable look ahead distance (scheduled vs. tether length) is travelled over the flight path to

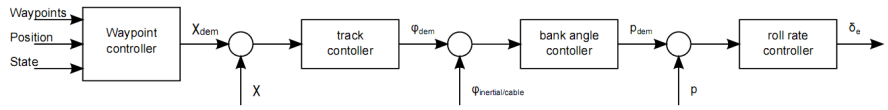

Fig. 10 Block diagram indicating the functioning of the lateral control scheme.

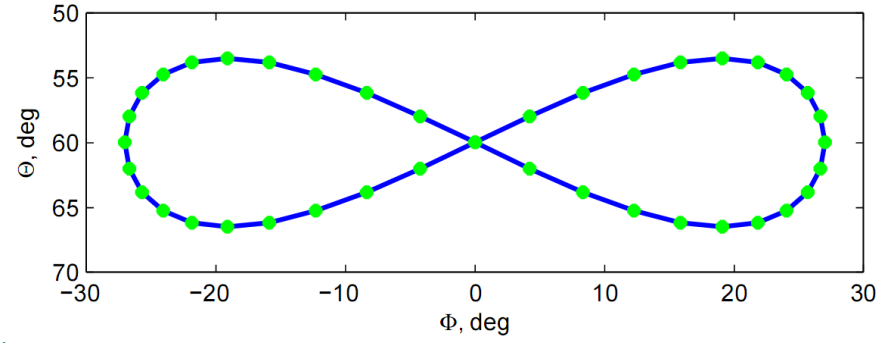

Fig. 11 Scheduled waypoints during the power generation phase in tether angles

determine a so called look ahead point. The direction toward this look ahead point is the track demand. A controller transforms the track error into a roll angle reference and the error thereof is by means of a PD controller transformed into a roll rate, Fig. 10.

The difference between phases lies in the waypoint scheduling governed by a waypoint controller and the roll angle selection (Euler vs tethered Euler). During power generation the gliders flight path is a lying figure of 8, Fig. 11. During the system reset it is a straight line starting at the location where the corresponding phase was activated and ending in the coordinates of pattern reentry.

4.3 State Machine

Since the maneuvering of the pumping kite system throughout an operational cycle, is too diverse to be governed by a single controller and or guidance scheme (cross-wind pattern flying during power generation vs. straight descending flight during system reset), a higher level supervision is required to switch between controllers. For the pumping kite system this task is fulfilled by a state machine. Depending on this state different controllers are active and others are reset.

Each state has a predefined set of criteria (flags, demands) that must be met to transition into a next state. Depending on the state, one or several transitions are possible. Furthermore in each state an abort can be triggered when exceeding the margins to the flight envelope, which triggers a completely independent control sys-

tem with its own state machine and consequent states and controllers to take over. Table 1 presents an overview of the relevant states for power generation.

Table 1 Pumping kit states used in power generation and corresponding criteria to complete the task of that state and trigger transition into a next state

State	Condition	Next state
Takeoff	Completed when reaching a set altitude and climb rate	Climb
Climb	Completed when reaching a set altitude	Pattern entry
Pattern entry	Completed when within a set range to the pattern	Power generation
Power generation	Completed when reaching a dynamically set tether length	Pattern exit
Pattern exit	Completed when reaching a set waypoint	Reset
Reset	Completed when reaching a minimum tether length	Pattern re-entry
Pattern re-entry	Completed when within a set range to the pattern	Power generation

5 Flight Performance of the Control System in Test Flights

The performance of the pumping kite system is illustrated by Figs. 12. The graphs present one complete power cycle starting in a reset phase, followed by a complete power generation phase and ends in the middle of another reset phase. The tether tension and speed, the true airspeed and angle of attack, Euler angles and tether based position and attitude are presented.

Comparing tethered Euler angles to the conventional one illustrates the linearizing effect mentioned in Sec 4. The tethered pitch angle varies approximately 20°from -20°to 0°and the tethered roll angle varies within -10°to 30°. The large negative pitch angle that is observed is due to the system being reset, where the plane flies toward the winch. With the tether being much longer than the flight altitude, this results in large negative pitch angles.

The angle of attack is tracked satisfactory in the beginning (to within plus or minus 1°). In the middle some oscillations are observed that however dampen out toward the end of the phase. Note that the oscillations in angle of attack have a strong correlation to the tether tension, but much less to the glider airspeed.

The flight path tracking performance is good. What is observable is the plane cutting the turns and staying within the flight path, which is a consequence of the waypoint tracking algorithm fixing the track demand to a location ahead on the set flight path. The strong overshoot is the spherical representation of the reset phase, where the plane flies toward the winch but does not sink as fast as the pattern would, resulting in a high entry into the pattern.

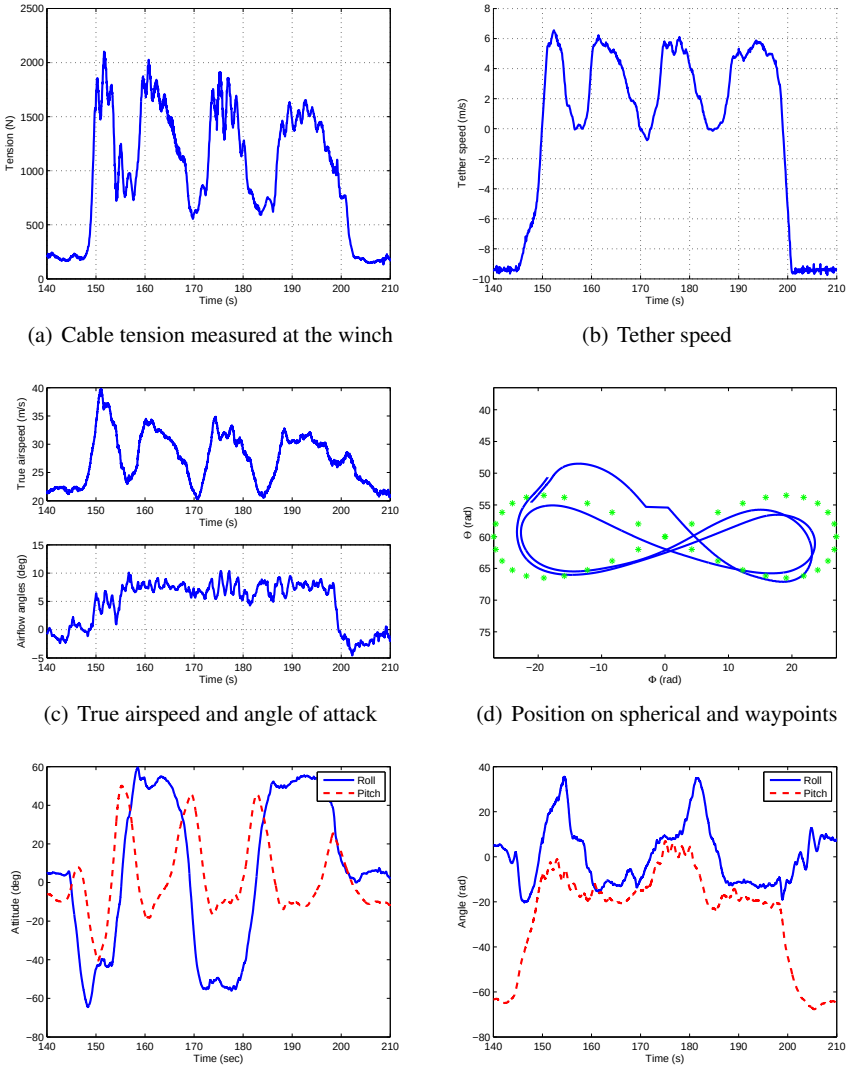

(a) Cable tension measured at the winch

(b) Tether speed

(c) True airspeed and angle of attack

(d) Position on spherical and waypoints

(e) glider Euler angles

(f) Tethered Euler angles

Fig. 12 Test results of one power cycle at 7 m/s wind speed, measured at 6.5 m reference height. Starting point of the graphs is the reset phase, followed by power generation and ending in another reset phase.

6 Conclusions

Through choosing the tether based reference frame and carefully selecting control variables, simple control schemes are well capable of flying the highly aggressive

patterns of the pumping kite system. In lateral direction the glider is controlled by means of a waypoint controller that produces track demands. Tracking errors generate roll angle demands, which again are used to create roll rate demands each through linear controllers. The longitudinal motion is controlled by fixing the elevator and thereby fixing the lift coefficient and system lift to drag ratio in combination with a tension controller determining the tether velocity.

References

1. Diehl, M. and Houska, B.: Windenergienutzung mit schnell fliegenden Flugdrachen: eine Herausforderung für die Optimierung und Regelung - Wind Power via Fast Flying Kites: a Challenge for Optimization and Control. at-automatisierungstechnik (2009)
2. Houska, B. and Diehl, M.: Optimal Control for Power Generating Kites. Proc. 9th European Control Conference (2007)
3. Loyd, M. L.: Crosswind Kite Power. J. of Energy (1980)
4. Manwell, J. F., McGowan, J. G. and Rogers, A. L.: Wind Energy Explained Theory, Design and Application. John Wiley and Sons, LTD, (2002)
5. Thresher, M., Robinson M. and Veers, P.: To Capture the Wind. IEEE Power and Energy Magazine (2007)
6. Williams, P., Lansdorp, B., and Ockels, W.: Optimal Cross-Wind Towing and Power Generation with Tethered Kites. J. of Guidance, Control and Dynamics, AIAA (2008).
7. Wortman, A. J.: Introduction to Wind Turbine Engineering. Butterworth (1982)
8. Sieberling, S., Ruiterkamp, R.: The PowerPlane an Airborne Wind Energy System Conceptual Operations. Proc. 11th AIAA ATIO Conference (2011)